Bridge Model Updating Using Response Surface Method and Genetic Algorithm

Lu Deng, A.M.ASCE[1]; and C. S. Cai, P.E., F.ASCE[2]

Abstract: A finite-element (FE) model of a structure is a highly idealized engineering model that may or may not truly reflect the physical structure. The purpose of model updating is to modify the FE model of a structure in order to obtain better agreement between the numerical and field-measured structure responses. In this paper, a new practical and user-friendly FE model updating method is presented. The new method utilizes the response surface method for the best experimental design of the parameters to be updated based on which numerical analysis can be performed in order to obtain explicit relationships between the structural responses and parameters from the simulation results. The parameters are then be updated using the genetic algorithm (GA) by minimizing an objective function. A numerical example of a simply supported beam has been used to demonstrate the concept. This method has also been applied to the model updating of an existing bridge. Results show that this method works well and achieves reasonable physical explanations for the updated parameters.

DOI: 10.1061/(ASCE)BE.1943-5592.0000092

CE Database subject headings: Finite element method; Structure response; Algorithms; Bridges.

Author keywords: Finite-element model; Model updating; Structure response; Response surface method; Genetic algorithm; Regression.

Introduction

Finite-element (FE) models play a very important role in the field of structural engineering because they can be used to predict the performance of structures. The FE model of a structure is a highly idealized engineering model that may or may not truly reflect the physical structure due to two possible factors, namely, modeling errors as a result of simplifications and/or assumptions made in the modeling process and uncertainties in material and geometric properties as well as boundary conditions (Lee et al. 1987; Mazurek and DeWolf 1990; Salawu and Williams 1995). The purpose of model updating is to modify the FE model of a structure in order to obtain better agreement between the numerical and field-measured structural responses.

A comprehensive review of the FE model updating techniques and their applications to damage detection was reported by Doebling et al. (1998). Generally, two types of methods have been used for model updating. The noniterative methods directly update the elements of stiffness and mass matrices in one step (Baruch and Bar-Itzhack 1978; Berman and Nagy 1983). The iterative parameter-updating methods use the sensitivity matrix of the updating parameters (Friswell and Mottershead 1995; Link 1999). Eigenvalue and eigenvector (natural frequencies and mode shapes) residuals are the most frequently used structural responses for model updating (Brownjohn and Xia 2000; Zhang et al. 2001; Xia and Brownjohn 2004). Residual from modal curvature or flexibility (Wahab 2001) and the modal assurance criterion related function (Teughels et al. 2001) have gained their popularity recently (Brownjohn and Xia 2000; Wu and Li 2004; Jaishi and Ren 2005). Static responses including deflection and strain have also been used in the objective function for the reason that performing a static test is usually much simpler and more economical than performing a dynamic test (Hajela and Soeilo 1990; Sanayei et al. 1997).

Marwala (2004) first introduced the use of response surface method (RSM) to structural model updating. In his study, the multilayer perceptron (MLP) is used to approximate the implicit function between the response and parameters. While the MLP makes the function less expensive to evaluate and can achieve accuracy of the same order as those given by the simulated annealing and genetic algorithm (GA) in his study, there are also problems with the use of the MLP. First, as a type of neural networks, the accuracy of MLP depends on many factors such as the number of layers in the model, the number of units in each layer, the samples, and the number of samples used in the training process. Also, it is difficult to interpret the relationships between the response and the parameters since there is no direct relationship between them due to the use of hidden units in the MLP.

In this study, a new, practical, and user-friendly FE model updating method is presented. The new method uses the RSM for the best experimental design of the parameters to be updated. Numerical analyses are then performed in order to obtain the direct explicit relationships between the structural responses and parameters from the simulation results. This could not be achieved by the MLP used in the study of Marwala (2004). The parameters are updated using the GA by minimizing an objective function built up using the residuals between the measured struc-

[1]Research Assistant, Dept. of Civil and Environmental Engineering, Louisiana State Univ., Baton Rouge, LA 70803.

[2]Edwin B. and Norma S. McNeil Distinguished Professor, Dept. of Civil and Environmental Engineering, Louisiana State Univ., Baton Rouge, LA 70803 (corresponding author). E-mail: cscai@lsu.edu

Note. This manuscript was submitted on April 18, 2008; approved on June 3, 2009; published online on November 27, 2009. Discussion period open until February 1, 2011; separate discussions must be submitted for individual papers. This paper is part of the ***Journal of Bridge Engineering***, Vol. 15, No. 5, September 1, 2010. ©ASCE, ISSN 1084-0702/2010/5-553–564/$25.00.

tural responses and the predicted responses from the expressed relationships. Natural frequencies from modal analysis and strains/deflections from static tests are used as responses in the objective function. A numerical example of a simply supported beam has been used to demonstrate the procedure. The proposed method has also been applied to the model updating of an existing bridge. Results show that this method works well and achieves reasonable physical explanations for the updated parameters which could be difficult to interpret when using the MLP proposed in Marwala's (2004) study.

RSM

In experimental design, reducing the number of samples usually plays a critical role in reducing the design cost. The factorial experimental design method is the most commonly used one. For a full factorial experiment, as the number of factors increases, the number of factorial points will increase dramatically. A fractional factorial design is an experimental design consisting of a carefully chosen subset (fraction) of the experimental runs of a full factorial design. However, for both the full factorial design and the fractional factorial design, usually only two levels of values are used for each factor. One limitation of the two-level factorial designs where the factors are quantitative is that they cannot identify curvatures in the response surface. Modeling curvature effects can be very important when the objective of the experiment is to identify the combination of levels of the quantitative factors that leads to an optimum response.

The RSM is an approximation optimization method that seeks the best experimental design using the minimum number of design samples. It was introduced into the field of experimental design in the late 1990s. RSM is a much more experimentally efficient way to determine the relationship between the experimental response and factors at multiple levels. It has been used in many engineering fields (Das and Zheng 2000; Wang et al. 2005; Landman et al. 2007). In civil engineering, the RSM has been used mainly in structural safety and reliability analysis (Bucher and Bourgund 1990; Das and Zheng 2000; Zheng and Das 2000; Cheng et al. 2005; Cheng et al. 2007).

The basic idea of the RSM is to use the so-called response surface function (RSF) to approximate the actual state function, which is usually implicit and difficult to express. Regression is usually performed to determine the RSF by the least-squares method (LSM). The RSF commonly takes the form of polynomials of the variables under consideration and is much easier to deal with than the actual state function. A quadratic form is often used for the RSF. Higher-order polynomials are generally not used for conceptual as well as computational reasons. A typical quadratic form for a response surface with three variables can be written as

$$Y = b_0 + b_1x_1 + b_2x_2 + b_3x_3 + b_{12}x_1x_2 + b_{13}x_1x_3 + b_{23}x_2x_3 + b_{11}x_1^2 + b_{22}x_2^2 + b_{33}x_3^2 \quad (1)$$

where Y=response and x_1, x_2, and x_3=variables.

Central composite designs (CCDs) are the most commonly used type of RSM designs. By adding a single center point and four star points to a full two-factor factorial design, a two-factor CCD can be obtained (Fig. 1). A star point is one in which all factors but one are set at their midlevels. The distance from a star point to the center point in code units is typically denoted by α. For designs that have k ($k \geq 3$) factors, the CCDs generally consist of three components (Kutner et al. 2004).

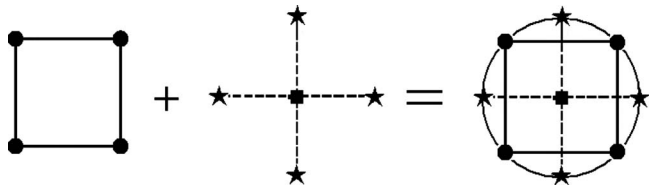

Fig. 1. Two-factor CCD

1. 2^{k-f} corner points. Here, f describes the size of the fraction of the full factorial design used. At the base of any CCD is a two-level full factorial design or a fractional factorial design. This component provides information for the estimation of linear main effects and all two-factor interaction effects. Corner points have coded coordinates of the form of $(\pm 1, \pm 1, \ldots \pm 1)$.
2. $2k$ star points. These factor level combinations permit the estimation of all quadratic main effects. In addition, when $\alpha = \sqrt[4]{2^k} \geq 1.0$, significance tests for higher-order curvature effects can be conducted. Star points have coded coordinates $(\pm\alpha, 0, \ldots, 0)$, $(0, \pm\alpha, \ldots, 0)$, etc., with one coordinate being $\pm\alpha$ and all other coordinates being zeros.
3. n_0 center points. Here, the case $n_0 \geq 1$ is possible and the coded coordinates of the center point replicates are $(0, 0, \ldots, 0)$.

Table 1 shows a three-factor CCD with four replicates at the center point, which will be used later in the simulation study. It should be noted that the CCD design shown in Table 1 is a standard design form for a case with three factors. The reason the center point is repeated four times is because the information at the center point is more important to the response surface compared with other points and using four replicates in the CCD design can help achieve a larger (yet reasonable) impact of the center point on the response surface than the other points. A list of widely used CCDs is also given in Table 2 for studies involving two to eight factors.

Table 1. Three-Factor CCD

	Factor level settings		
Experimental trial number	X1	X2	X3
1 (corner point)	−1	−1	−1
2 (corner point)	1	−1	−1
3 (corner point)	−1	1	−1
4 (corner point)	1	1	−1
5 (corner point)	−1	−1	1
6 (corner point)	1	−1	1
7 (corner point)	−1	1	1
8 (corner point)	1	1	1
9 (star point)	−α	0	0
10 (star point)	α	0	0
11 (star point)	0	−α	0
12 (star point)	0	α	0
13 (star point)	0	0	−α
14 (star point)	0	0	α
15 (center point)	0	0	0
16 (center point)	0	0	0
17 (center point)	0	0	0
18 (center point)	0	0	0

Table 2. CCDs for Different Number of Factors

	Number of Factors						
	2	3	4	5	6	7	8
Base factorial design	2^2	2^3	2^4	2^{5-1}	2^{6-1}	2^{7-1}	2^{8-2}
Star points	4	6	8	10	12	14	16
Center point replicate	4	4	4	4	4	4	4
α	1.4142	1.6818	2	2.3784	2.8284	3.3636	4
Total number of trials	12	18	28	30	48	82	84

GA

GAs (Goldberg 1989; Gen and Cheng 1997) are stochastic global search techniques based on the mechanics of natural selection and natural genetics. They are widely applied in bioinformatics, phylogenetics, computer science, engineering, economics, chemistry, manufacturing, mathematics, physics, and other fields. GAs are implemented to an optimization problem as a computer simulation in which a population of abstract representations (usually called chromosomes) of candidate solutions (usually called individuals, creatures, or phenotypes) evolves toward better solutions. The evolution usually starts from a population of randomly generated individuals and continues in new generations. In each generation, the fitness of every individual in the population is evaluated, multiple individuals are stochastically selected from the current population based on their fitness, and the population is modified (recombined and possibly randomly mutated) to form a new population. The new population is then used in the next iteration of the algorithm. Commonly, the algorithm terminates when either a maximum number of generations has been produced or a satisfactory fitness level has been reached for the population.

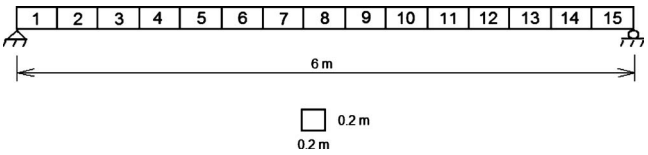

Fig. 2. Simply supported concrete beam under study

Simulation Study

A simulated, simply supported, concrete beam is taken as an example to demonstrate how the proposed RSM and GA can be used in FE model updating. Fig. 2 shows the concrete beam under study, which is divided into 15 elements. The beam has a length of 6 m with a cross section of 0.2 m by 0.2 m. Originally, Young's modulus, Poisson's ratio, and the density of the concrete are assumed to be 20 GPa, 0.3, and $2,400\ \text{kg/m}^3$, respectively.

In the numerical simulation, it is assumed that the beam is either damaged or has a stiffness change due to any other reasons at the position of elements 4 and 8. The true values of Young's modulus for elements 4 and 8 are 15 and 12 GPa, respectively. Also, the real density of the concrete is $2,200\ \text{kg/m}^3$. The proposed method is then applied to update this beam model and find out the true values for the three parameters, i.e., the Young's modulus for both elements 4 and 8 and the real density of the concrete beam.

The CCD shown in Table 1 is used for this three-factor experimental design. Based on the assumption that damages have occurred at elements 4 and 8, the baseline values for the Young's modulus of these two elements are taken as 20 GPa. The baseline value for the density of concrete beam is taken as $2,400\ \text{kg/m}^3$.

Table 3. Experimental Design for the Beam Example and Simulated Results for the Responses

Trial number	X1 (GPa)	X2 (GPa)	X3 (10^3 kg/m^3)	Freq. 1 (Hz)	Freq. 2 (Hz)	Freq. 3 (Hz)	Strain (μ)
1	10	10	1.920	8.515	14.027	35.879	12.264
2	30	10	1.920	8.901	14.091	39.938	12.261
3	10	30	1.920	9.432	15.174	36.069	11.983
4	30	30	1.920	9.971	15.201	39.997	11.980
5	10	10	2.880	6.952	11.453	29.295	12.264
6	30	10	2.880	7.268	11.505	32.609	12.261
7	10	30	2.880	7.701	12.389	29.450	11.983
8	30	30	2.880	8.141	12.412	32.658	11.980
9	3	20	2.400	7.138	13.204	27.122	12.093
10	37	20	2.400	8.687	13.307	36.209	12.088
11	20	3	2.400	6.190	10.918	34.464	12.455
12	20	37	2.400	8.896	13.710	34.706	11.928
13	20	20	1.593	10.462	16.318	42.571	12.089
14	20	20	3.207	7.372	11.500	30.000	12.089
15	20	20	2.400	8.523	13.294	34.680	12.089
16	20	20	2.400	8.523	13.294	34.680	12.089
17	20	20	2.400	8.523	13.294	34.680	12.089
18	20	20	2.400	8.523	13.294	34.680	12.089

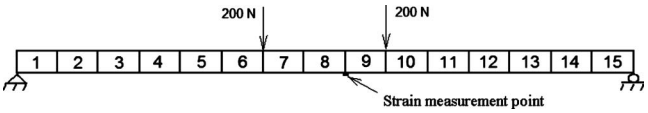

Fig. 3. Static test on the beam

Assuming a unit change for each of the three parameters to be 50, 50, and 20% of the baseline values, respectively, a detailed CCD for the three parameters can be obtained and is shown in the first four columns in Table 3. As can be seen from the table, a combination of properly chosen baseline values and unit changes for the three parameters can generate a reasonable range that is able to cover almost all possible values for each parameter.

Numerical modal tests and static tests are then performed on the beam based on the CCD in Table 3. In the static test, the beam is subjected to two concentrated loads of 200 N as shown in Fig. 3. The first three natural frequencies from the modal analysis and the strain at the bottom of the section near the midspan of the beam from the static test are obtained as responses. Simulated results for the responses are shown in the last four columns in Table 3. Based on the parameters and the corresponding responses, regression is performed to determine the RSFs through LSM. The obtained second-order RSFs for the four responses can be expressed as follows:

$$Y_1 = 13.6369 + 0.0988x_1 + 0.1916x_2 - 5.6282x_3 + 0.0003x_1x_2 - 0.0044x_1x_3 - 0.0095x_2x_3 - 0.0016x_1^2 - 0.0029x_2^2 + 0.8506x_3^2 \quad (2)$$

$$Y_2 = 23.2057 - 0.0007x_1 + 0.2193x_2 - 7.7700x_3 - 0.0001x_1x_2 - 0.0004x_1x_3 - 0.0108x_2x_3 - 0.0001x_1^2 - 0.0032x_2^2 + 1.0667x_3^2 \quad (3)$$

Table 5. Identified Values for the Three Parameters Using Third-Order RSFs

Parameters	True value	Identified value	Error (%)
X1 (GPa)	15.000	14.667	−2.22
X2 (GPa)	12.000	12.065	0.55
X3 (10^3 kg/m^3)	2.200	2.180	−0.91

$$Y_3 = 58.3371 + 0.7126x_1 - 0.0008x_2 - 20.0522x_3 - 0.0003x_1x_2 - 0.0382x_1x_3 - 0.0012x_2x_3 - 0.0099x_1^2 - 0.0004x_2^2 + 2.7835x_3^2 \quad (4)$$

$$Y_4 = 12.5276 + 0.0001x_1 - 0.0290x_2 + 0.0000x_3 + 0.0000x_1x_2 + 0.0000x_1x_3 + 0.0000x_2x_3 + 0.0000x_1^2 + 0.0000x_2^2 - 0.0000x_3^2 \quad (5)$$

where Y_1, Y_2, Y_3, and Y_4 denote the four responses, i.e., the first, second, and third natural frequencies of the beam and the strain at the bottom of the section near the midspan of the beam from the static test, respectively; the three variables x_1, x_2, and x_3 represent the three parameters, i.e., Young's modulus of element 4, the Young's modulus of element 8, and the density of the concrete, respectively. The units for the responses and parameters are the same as those in Table 3.

An objective function is then built up using the residuals between the measured (or true) responses and the predicted responses from the RSFs. In numerical simulation without physical tests, the results based on the true parameters (15 GPa, 12 GPa, and 2,200 kg/m^3) are used to represent the measured response.

Based on the true results for the first three natural frequencies and the strain near the midspan of the beam from the static test, which are 8.3279, 13.3550, 35.2020 Hz, and 12.2210μ, respectively, the objective function can be written as follows:

$$F_{obj} = \sqrt{(Y_1 - 8.3279)^2 + (Y_2 - 13.3550)^2 + (Y_3 - 35.2020)^2 + (Y_4 - 12.2210)^2} \quad (6)$$

It should be noted that the magnitude of two concentrated loads in the static test will affect the magnitude of the resultant strain at the midspan and therefore the weight of the strain information in the objective function in Eq. (6) since no weight coefficient was given for the four residual terms in Eq. (6). The reason why no weight coefficient was assigned for these residual terms was because in this simulation example, the use of weight coefficients has little effect on the accuracy of the identified parameters, as can be seen by the identified parameters later. However, the best way to eliminate the effect of the load magnitude is to

Table 4. Identified Values for the Three Parameters Using Second-Order RSFs

Parameters	True value	Identified value	Error (%)
X1 (GPa)	15.000	15.898	5.99
X2 (GPa)	12.000	13.598	13.31
X3 (10^3 kg/m^3)	2.200	2.188	−0.55

Table 6. Identified Values for the Three Parameters Using Four Different Objective Functions

Objective function	Parameters	True value	Identified value	Error (%)
F_{obj}_1	X1 (GPa)	15.000	19.871	32.47
	X2 (GPa)	12.000	31.994	166.62
	X3 (10^3 kg/m^3)	2.200	2.657	20.78
F_{obj}_2	X1 (GPa)	15.000	26.011	73.40
	X2 (GPa)	12.000	11.938	−0.52
	X3 (10^3 kg/m^3)	2.200	2.224	1.08
F_{obj}_3	X1 (GPa)	15.000	14.596	−2.70
	X2 (GPa)	12.000	12.470	3.92
	X3 (10^3 kg/m^3)	2.200	2.200	0
F_{obj}_4	X1 (GPa)	15.000	14.667	−2.22
	X2 (GPa)	12.000	12.065	0.55
	X3 (10^3 kg/m^3)	2.200	2.180	−0.91

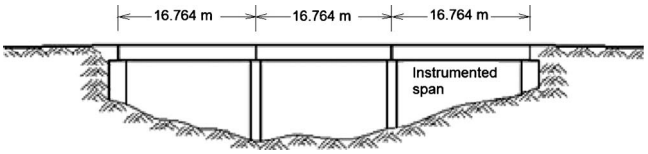

Fig. 4. Profile of the test bridge

conduct a sensitivity study and use a weight coefficient for each residual term in the objective function based on their relative importance, as will be shown later in Eq. (17) for the field study.

By defining the lower and upper bounds for each of the parameters in the objective function, which are set to be [0 GPa; 0 GPa; 2,000 kg/m^3] and [40 GPa; 40 GPa; 2,800 kg/m^3] in this case, F_{obj} can be optimized using the GA. The identified values for the three parameters obtained using the GA as well as the differences from their true values are listed in Table 4.

As can be seen from the table, the errors for the Young's modulus of element 4 and the density of the concrete are both under 6%, which is acceptable. However, the error for Young's modulus of element 8 reaches 13%, which is slightly too large. In order to find out the cause of the relatively large error and further improve the accuracy of the identified results, third-order RSFs with the cross-terms ignored are obtained for the four responses as follows:

$$Y_1 = 16.8841 + 0.2390x_1 + 0.3894x_2 - 11.8340x_3 + 0.0003x_1x_2 - 0.0044x_1x_3 - 0.0095x_2x_3 - 0.0098x_1^2 - 0.0145x_2^2 + 3.4985x_3^2 + 0.0001x_1^3 + 0.0002x_2^3 - 0.3678x_3^3 \quad (7)$$

$$Y_2 = 28.1998 + 0.0048x_1 + 0.3971x_2 - 15.3815x_3 - 0.0001x_1x_2 - 0.0004x_1x_3 - 0.0108x_2x_3 - 0.0002x_1^2 - 0.0136x_2^2 + 4.3142x_3^2 + 0.0000x_1^3 + 0.0002x_2^3 - 0.4510x_3^3 \quad (8)$$

$$Y_3 = 72.3280 + 1.2100x_1 + 0.0077x_2 - 41.3310x_3 + 0.0003x_1x_2 - 0.0382x_1x_3 - 0.0012x_2x_3 - 0.0391x_1^2 - 0.0001x_2^2 + 11.8620x_3^2 + 0.0005x_1^3 + 0.0000x_2^3 - 1.2609x_3^3 \quad (9)$$

$$Y_4 = 12.5673 + 0.0001x_1 - 0.0380x_2 + 0.0000x_3 + 0.0000x_1x_2 + 0.0000x_1x_3 + 0.0000x_2x_3 + 0.0000x_1^2 + 0.0009x_2^2 - 0.0000x_3^2 + 0.0000x_1^3 + 0.0000x_2^3 + 0.0000x_3^3 \quad (10)$$

The same procedures are implemented again to identify the three variables, and the results are shown in Table 5.

Comparing the results in Tables 4 and 5, it is clear that the accuracy of identified result for the Young's modulus of element 8 has been greatly improved. For the Young's modulus of element 4, the accuracy of the identified result is also improved. It can therefore be concluded that in this case, third-order RSFs can better represent the real relationships between the responses and parameters and can therefore produce better identification results. It is noted that in a real application, the real parameter values are usually not available; however, as shown later in the field bridge example, comparison can always be made between the prediction using the updated model and the measurements. If the difference is not acceptable, the model can be further improved by adding more terms and/or more parameters.

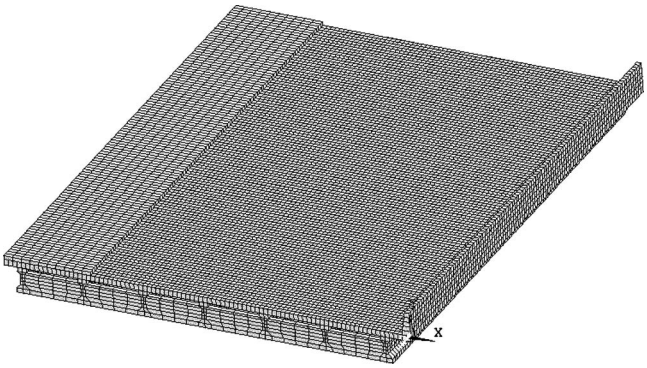

Fig. 5. Numerical model of the bridge under study

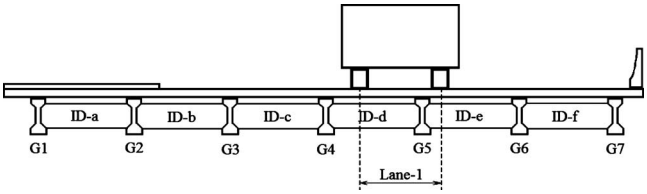

Fig. 6. Static test performed on the bridge

In order to find out how many responses would be enough to identify the three parameters accurately, a series of studies have been carried out. Four different objective functions have been built up using one, two, three, or all four responses, respectively, as shown below

$$F_{obj\_}1 = \sqrt{(Y_1 - 8.3279)^2} \quad (11)$$

$$F_{obj\_}2 = \sqrt{(Y_1 - 8.3279)^2 + (Y_4 - 12.2210)^2} \quad (12)$$

$$F_{obj\_}3 = \sqrt{(Y_1 - 8.3279)^2 + (Y_2 - 13.3550)^2 + (Y_4 - 12.2210)^2} \quad (13)$$

$$F_{obj\_}4 = \sqrt{(Y_1 - 8.3279)^2 + (Y_2 - 13.3550)^2 + (Y_3 - 35.2020)^2 + (Y_4 - 12.2210)^2} \quad (14)$$

The four objective functions can be optimized using the GA and the identified results for the three parameters are shown in Table 6.

As can be seen from the table, using only one or two responses in the objective function gives poor results, with the largest error reaching 167% when using one response and 73% when using two responses. However, using three or four responses can significantly reduce the error in the identified results, with all errors below 4%. It may be concluded that the number of responses needed in the objective function should be at least no less than the number of parameters to be identified.

It should be noted in this numerical example that the locations of damages were assumed to be known and only three parameters were selected for identification. In reality, if the locations of dam-

Table 7. Experimental Design of the Five Parameters Using the RSM

	Factor level setting				
Trial number	X1	X2	X3	X4	X5
1	−1	−1	−1	−1	1
2	1	−1	−1	−1	−1
3	−1	1	−1	−1	−1
4	1	1	−1	−1	1
5	−1	−1	1	−1	−1
6	1	−1	1	−1	1
7	−1	1	1	−1	1
8	1	1	1	−1	−1
9	−1	−1	−1	1	−1
10	1	−1	−1	1	1
11	−1	1	−1	1	1
12	1	1	−1	1	−1
13	−1	−1	1	1	1
14	1	−1	1	1	−1
15	−1	1	1	1	−1
16	1	1	1	1	1
17	−2	0	0	0	0
18	2	0	0	0	0
19	0	−2	0	0	0
20	0	2	0	0	0
21	0	0	−2	0	0
22	0	0	2	0	0
23	0	0	0	−2	0
24	0	0	0	2	0
25	0	0	0	0	−2
26	0	0	0	0	2
27	0	0	0	0	0
28	0	0	0	0	0
29	0	0	0	0	0
30	0	0	0	0	0

ages for a large-scale and complex structure are unknown, it can be a challenging task to identify the parameters using the proposed method. As a matter of fact, because of the complex nature of parameter identification, it has never been an easy task for engineers to accurately identify the parameters of a real structure. Instead, as will be demonstrated later in the field study, assumptions are usually made, based on our best knowledge, to simplify the complicated real situation.

Model Updating of an Existing Bridge

The proposed method has also been applied to the model updating of an existing bridge. The tested bridge is a two-way bridge located over Cypress Bayou in District 61, on LA 408 East, Louisiana. This bridge is representative of a large majority of prestressed concrete slab-on-girder highway bridges in the United States. It consists of two separated structures, which are identical and symmetric about the center line of the bridge. Each structure provides a path for traffic traveling in one direction. Since they are separated, only one structure has been investigated in this study.

The bridge structure considered in this study has three straight, simple spans, each measuring 16.764 m (55 ft) in length with zero skew angles (Fig. 4). Seven AASHTO type-II prestressed concrete girders, spaced 2.13 m (7 ft) from center to center, are used for the bridge. All girders are supported by rubber bearings at both ends. Each span has one intermediate diaphragm located at the midspan and two more located at both ends of the span, all of which are separated from the bridge deck.

The third span of the bridge was instrumented. A total of seven measurement stations (S1, S2, S3, S4, S5, S6, and S7 corresponding to girders G1, G2, G3, G4, G5, G6, and G7) were selected, each with a distance of 0.305 m (1 ft) from the midspan of the corresponding girder to avoid stress concentration near the diaphragm. Strain gauges, accelerometers, and cable extension transducers were placed at each of the seven stations.

Based on the configuration of the bridge, a numerical model was created using the ansys program (Fig. 5). The bridge deck, girders, diaphragms, shoulder, and railing are all modeled using the solid elements, which have three translational DOFs for each node. Since the prestressing force effect on vibration frequencies of concrete beams and bridges has been studied by some researchers (Saiidi et al. 1994; Hamed and Frostig 2006) and controversy still exists concerning whether prestressing tends to decrease the natural frequencies or has a negligible effect, in this study, the prestressing force effect is taken into consideration by modifying Young's modulus of the concrete girders in the model updating process. The rubber bearings are modeled using equiva-

Table 8. Experimental Design Values for the Five Parameters

	Factor values				
Trial number	X1 (GPa)	X2 (GPa)	X3 (10^3 kg/m^3)	X4 (GPa)	X5 (MPa)
1	18.000	21.000	1.920	12.000	70.000
2	42.000	21.000	1.920	12.000	30.000
3	18.000	49.000	1.920	12.000	30.000
4	42.000	49.000	1.920	12.000	70.000
5	18.000	21.000	2.880	12.000	30.000
6	42.000	21.000	2.880	12.000	70.000
7	18.000	49.000	2.880	12.000	70.000
8	42.000	49.000	2.880	12.000	30.000
9	18.000	21.000	1.920	28.000	30.000
10	42.000	21.000	1.920	28.000	70.000
11	18.000	49.000	1.920	28.000	70.000
12	42.000	49.000	1.920	28.000	30.000
13	18.000	21.000	2.880	28.000	70.000
14	42.000	21.000	2.880	28.000	30.000
15	18.000	49.000	2.880	28.000	30.000
16	42.000	49.000	2.880	28.000	70.000
17	6.000	35.000	2.400	20.000	50.000
18	54.000	35.000	2.400	20.000	50.000
19	30.000	7.000	2.400	20.000	50.000
20	30.000	63.000	2.400	20.000	50.000
21	30.000	35.000	1.440	20.000	50.000
22	30.000	35.000	3.360	20.000	50.000
23	30.000	35.000	2.400	4.000	50.000
24	30.000	35.000	2.400	36.000	50.000
25	30.000	35.000	2.400	20.000	10.000
26	30.000	35.000	2.400	20.000	90.000
27	30.000	35.000	2.400	20.000	50.000
28	30.000	35.000	2.400	20.000	50.000
29	30.000	35.000	2.400	20.000	50.000
30	30.000	35.000	2.400	20.000	50.000

lent beam elements with six DOFs (three translational and three rotational) for each node and a rigid connection is assumed between the rubber bearings and the supports. A rigid connection has also been assumed between both girders and diaphragms and between girders and the bridge deck. It should be noted that since the damping coefficients of the bridge were difficult to obtain, in this study, a damping coefficient of 2% was assumed for all modes considered.

Because of their uncertainty, five parameters are selected as variables. The five parameters are Young's modulus of the concrete for the bridge deck, the seven girders, the diaphragms, the density of the bridge deck, and the stiffness of the rubber bearing. In the original model, the density of the concrete was taken as 2,323 kg/m^3, Young's modulus for the rubber bearings was taken as 200 MPa [266.6 MPa is used in the LRFD specifications by AASHTO (1998)], and Young's modules used for concrete were 25.12 GPa for both the bridge deck and diaphragms and 32.03 GPa for the seven girders, all of which were calculated from the equation below (AASHTO 2004) using a design strength of 44.82 MPa for the girders and 27.58 MPa for both the bridge deck and diaphragms

$$E_0 = w_c^{1.5}(0.043)\sqrt{f'_c} \tag{15}$$

where w_c=density and f'_c=design strength of the concrete, respectively.

Both dynamic and static tests (Fig. 6) were performed on the bridge. For the static test, a loaded truck drove on the bridge along lane 1 at a crawling speed (less than 2 m/s), and the bridge responses on all the seven girders were recorded in time history. In the dynamic test, the loaded truck is driven to the bridge with a given speed. Modal analysis was done using the free vibration response of the bridge from the dynamic test when the truck was off the bridge and the first three natural frequencies were obtained.

To obtain the relationship between the responses and the selected parameters, the RSM is first used for the experimental design. A fractional design with five factors, each with five levels, has been used for the experimental design in this study. Table 7 shows the details of this fractional design, where X1, X2, X3, X4, and X5 represent Young's modulus of the bridge girders, Young's modulus of the bridge deck, the density of the bridge deck concrete, Young's modulus of the diaphragms, and the equivalent Young's modulus of the bearings.

The baseline values are usually chosen near the original estimates based on construction drawings. However, to improve accuracy, they can be adjusted for more realistic values after some analyses. Therefore, the five parameters are taken as 30 GPa, 35 GPa, 2,400 kg/m^3, 20 GPa, and 50 MPa based on a preliminary study of the parameters, with the bearing modulus (50 MPa) significantly different from the original estimate (200 MPa). The

Table 9. Results for the Responses from Simulation

Trial number	R(1) (Hz)	R(2) (Hz)	R(3) (Hz)	R(4) (μ)	R(5) (μ)	R(6) (μ)	R(7) (μ)	R(8) (μ)	R(9) (μ)	R(10) (μ)
1	7.901	10.679	16.412	−1.289	10.490	26.190	51.140	59.810	39.730	16.430
2	7.575	11.367	15.359	−0.239	10.270	23.940	46.630	55.340	36.860	15.060
3	7.838	11.041	16.372	−0.773	5.121	13.160	27.530	32.750	21.330	8.378
4	10.622	13.948	21.036	−0.963	3.899	10.930	24.560	29.880	18.600	5.739
5	6.083	8.694	12.906	−0.852	11.120	26.660	51.060	59.660	40.380	17.670
6	7.740	10.636	16.396	−0.659	9.715	23.550	46.640	55.350	36.280	14.090
7	8.155	10.589	15.915	−0.950	4.587	12.560	27.230	32.490	20.590	7.412
8	7.401	11.133	14.753	−0.798	4.384	11.450	24.850	30.170	19.280	6.536
9	6.983	11.168	14.843	1.582	12.540	26.550	45.420	51.660	38.090	22.180
10	8.888	13.347	18.843	1.033	10.930	23.560	42.030	48.570	34.000	16.990
11	9.356	13.309	21.039	−0.051	5.658	13.110	23.820	27.240	19.250	10.040
12	8.513	14.206	16.844	−0.103	5.191	11.850	22.160	25.900	17.940	8.389
13	6.924	10.305	15.547	0.986	12.010	26.230	45.440	51.650	37.430	20.930
14	6.622	11.090	13.455	1.518	11.410	23.880	42.080	48.700	34.580	17.940
15	6.844	10.794	14.362	0.293	6.115	13.540	24.070	27.530	19.950	11.060
16	9.291	13.280	19.715	−0.365	4.765	11.430	21.880	25.570	17.300	7.572
17	6.389	9.281	14.520	0.626	9.755	21.420	36.290	40.750	30.620	18.860
18	8.902	13.105	18.267	−0.356	6.258	14.830	28.830	34.080	22.760	9.370
19	5.598	9.180	11.581	10.820	32.460	62.600	0.000	0.000	87.740	47.220
20	9.121	12.879	19.267	−0.526	3.867	9.761	19.870	23.500	15.480	6.242
21	9.788	13.979	20.815	−0.511	6.671	16.000	30.640	35.790	24.230	10.600
22	7.423	10.615	15.738	−0.511	6.671	16.000	30.640	35.790	24.230	10.600
23	8.339	10.415	14.906	−1.500	4.260	14.130	37.160	46.940	27.490	6.236
24	8.379	12.917	17.797	0.468	7.302	16.010	28.190	32.270	23.200	12.500
25	5.023	9.502	10.663	0.278	8.118	17.680	32.160	37.550	26.620	13.320
26	9.212	12.561	19.536	−0.705	6.391	15.780	30.650	35.830	23.920	10.050
27	8.367	11.953	17.766	−0.511	6.671	16.000	30.640	35.790	24.230	10.600
28	8.367	11.953	17.766	−0.511	6.671	16.000	30.640	35.790	24.230	10.600
29	8.367	11.953	17.766	−0.511	6.671	16.000	30.640	35.790	24.230	10.600
30	8.367	11.953	17.766	−0.511	6.671	16.000	30.640	35.790	24.230	10.600

Table 10. Updated Results for the Five Parameters

Parameter	X1 (GPa)	X2 (GPa)	X3 (kg/m^3)	X4 (GPa)	X5 (MPa)
Original estimate	25.12	32.03	2323	25.12	200
Updated	29.44	35.87	2693	10.07	53.5
Difference (%)	17.18	11.99	15.93	−59.91	−73.25

ranges for each parameter can be defined by assuming the value for a unit change of each parameter, which are taken as 40, 40, 20, 40, and 40% of the baseline values for the five parameters, respectively. The selection of these values is based on personal experience. The reason why a 20% change of the baseline value is taken as a unit change for the density of the concrete is because normally the density of the concrete will not change as much as the strength of the concrete. The density changes also reflect the additional mass of nonstructural members. Finally, the experimental design with designed values for the whole set of parameters is listed in Table 8.

According to the experimental design, numerical analysis is performed and bridge responses are obtained. Depending on the purpose of model updating, different bridge responses can be used in the model updating process. In this study, the bridge model was first updated with the purpose of achieving good agreement between the first three natural frequencies and the maximum strains on the girders from the static test. Numerical results of the responses are shown in Table 9, where R(1), R(2), and R(3) denote the first three natural frequencies of the bridge, respectively, and R(4), R(5), R(6), R(7), R(8), R(9), and R(10) represent the maximum strains at the seven measurement stations (from G1 to G7), respectively.

Regression has been performed to obtain the relationships between the responses and the parameters. A full second-order regression function has been used in the RSFs for all the responses. Results of the RSFs can be expressed in matrix form as follows:

$$R = A^T X \tag{16}$$

where R=response vector; X=variable vector; and A=coefficient. R and X can be expressed as follows:

$$R = \begin{Bmatrix} R(1) \\ R(2) \\ R(3) \\ R(4) \\ R(5) \\ R(6) \\ R(7) \\ R(8) \\ R(9) \\ R(10) \end{Bmatrix}; \quad X = \begin{Bmatrix} 1 \\ X1 \\ X2 \\ X3 \\ X4 \\ X5 \\ X1 \cdot X2 \\ X1 \cdot X3 \\ X1 \cdot X4 \\ X1 \cdot X5 \\ X2 \cdot X3 \\ X2 \cdot X4 \\ X2 \cdot X5 \\ X3 \cdot X4 \\ X3 \cdot X5 \\ X4 \cdot X5 \\ X1^2 \\ X2^2 \\ X3^2 \\ X4^2 \\ X5^2 \end{Bmatrix}$$

Matrix A can be written in the matrix form as follows:

$$A = \begin{bmatrix}
6.2314 & 8.4327 & 13.1110 & 3.5006 & 30.0555 & 66.0570 & 122.8600 & 143.6400 & 98.7830 & 47.0420 \\
0.0765 & 0.1265 & 0.0647 & 0.0616 & -0.0614 & -0.1827 & -0.1483 & -0.0609 & -0.1907 & -0.3363 \\
0.1003 & 0.1043 & 0.2586 & -0.4505 & -1.2275 & -2.3120 & -3.8426 & -4.3993 & -3.1674 & -1.7520 \\
-2.9719 & -3.7439 & -6.5834 & 0 & 0 & 0 & 0 & 0 & 0 & 0 \\
-0.0414 & 0.1076 & 0.0927 & 0.3529 & 0.4475 & 0.4247 & -0.3338 & -0.7301 & 0.0451 & 0.8590 \\
0.0826 & 0.0692 & 0.1406 & 0.0173 & 0.0160 & 0.0571 & 0.1467 & 0.1734 & 0.0793 & -0.0041 \\
0.0003 & 0.0005 & 0.0001 & -0.0007 & 0.0002 & 0.0015 & 0.0024 & 0.0024 & 0.0022 & 0.0017 \\
-0.0051 & -0.0099 & 0.0236 & 0 & 0 & 0 & 0 & 0 & 0 & 0 \\
-0.0001 & 0.0002 & -0.0019 & -0.0013 & -0.0006 & -0.0000 & 0.0024 & 0.0030 & 0.0001 & -0.0032 \\
0.0005 & 0.0001 & 0.0013 & 0.0001 & 0.0001 & 0.0000 & -0.0000 & -0.0001 & 0.0001 & 0.0002 \\
-0.0061 & -0.0081 & -0.0316 & 0 & 0 & 0 & 0 & 0 & 0 & 0 \\
-0.0001 & 0.0002 & 0.0013 & -0.0027 & -0.0009 & 0.0011 & 0.0046 & 0.0059 & 0.0021 & -0.0032 \\
0.0006 & 0.0003 & 0.0011 & 0.0002 & 0.0001 & -0.0001 & -0.0003 & -0.0003 & -0.0001 & 0.0002 \\
0.0081 & -0.0094 & 0.0117 & 0 & 0 & 0 & 0 & 0 & 0 & 0 \\
-0.0045 & -0.0026 & -0.0118 & 0 & 0 & 0 & 0 & 0 & 0 & 0 \\
-0.0000 & -0.0002 & 0.0021 & -0.0002 & 0.0001 & 0.0002 & -0.0000 & -0.0001 & 0.0000 & -0.0000 \\
-0.0009 & -0.0009 & -0.0016 & -0.0003 & 0.0002 & 0.0004 & -0.0020 & -0.0034 & -0.0004 & 0.0031 \\
-0.0010 & -0.0009 & -0.0024 & 0.0062 & 0.0131 & 0.0233 & 0.0379 & 0.0434 & 0.0315 & 0.0184 \\
0.4681 & 0.6190 & 1.0249 & 0 & 0 & 0 & 0 & 0 & 0 & 0 \\
0.0007 & -0.0002 & -0.0038 & -0.0032 & -0.0081 & -0.0111 & -0.0041 & 0.0009 & -0.0061 & -0.0115 \\
-0.0007 & -0.0004 & -0.0014 & -0.0010 & -0.0004 & -0.0007 & -0.0014 & -0.0017 & -0.0010 & -0.0004
\end{bmatrix}$$

The first three natural frequencies obtained from the modal analysis of the field bridge dynamic tests are 8.19, 11.11, and 15.79 Hz, respectively. The maximum strains at the seven measurement stations (from G1 to G7) obtained from the static test are −4, 6.5, 12, 32, 68, 23, and 2.5μ, respectively. An objective function can then be built as the summation of the weighted absolute residuals between the measured responses and the predicted responses from the RSFs, which is shown below:

$$F_{\text{obj}} = \sum_{i=1}^{10} \text{coef}(i) \times |R(i) - M(i)| \tag{17}$$

where $R(i)$=predicted response from the RSF; $M(i)$=corresponding measured response; and coef(i)=weight coefficient used to denote the importance level of each residual term $|R(i)-M(i)|$ in the objective function. The weight coefficients for different responses are usually determined based on the purpose of model updating. Therefore, different combinations of weight coefficients are possible. It should be noted that Eq. (17) uses a different form from the typical one used in Eq. (6). The main reason behind this change is the consideration of the relative weight of each residual term in the objective function. Since noise and error always exist in field measurements, taking a square of each residual term, as done in Eq. (6), may amplify the importance of some residual terms. A proper combination of weight coefficients can ensure that each residual term is treated according to its relative importance in the objective function.

In this study, coef is taken as [5 5 5 1 2 2 3 0 3 1] based on the results of a sensitivity study and personal judgment. The reason why the frequencies take larger weight coefficients than the strains is that they are less sensitive to the parameter changes than the strains; the strain from G5 takes a weight coefficient of 0 because of an obvious error with the measured data from G5; also, larger weight coefficients are taken for the girders closer to the lane where the truck travels because the data obtained from those girders are considered to be more reliable and important than those from other girders.

The objective function can then be optimized using the GA, with the lower and upper bounds for the five parameters set to be [15 GPa; 20 GPa; 1,800 kg/m^3; 0 GPa; 0 MPa] and [50 GPa; 60 GPa; 3,000 kg/m^3; 50 GPa; 400 MPa] based on personal judgment. The updated results of the five parameters and their differences from the original values are shown in Table 10.

Table 11. Reconstructed First Three Natural Frequencies

Natural frequencies	First	Second	Third
Measured	8.19	11.11	15.79
Reconstructed	8.19	10.79	16.23
Difference (%)	0	−2.9	2.8

As can be seen from the table, both Young's modulus of the bridge deck and girders have been increased, which is predictable because the strength of concrete increases with time and their initial cast strengths are usually higher than that specified in the construction drawings. The large decrease of Young's modulus of the diaphragms could be due to the fact that the diaphragms are not fully connected to the girders (Cai and Shahawy 2004), which can be observed from the field. Also, the small increase in the density of the bridge deck could be due to the addition of wearing surfaces, while the large decrease of Young's modulus of the rubber bearings could be due to the uncertain restraint condition of the bearing at the supports (Barker 2001). For example, in this case, the real connections between the rubber bearings and the supports are not rigid moment connections, with the rubber bearings able to move over the supports.

To verify the updated results for Young's modulus of the concrete, the strength of the concrete of the existing bridge was tested using a rebounding hammer. After conversion using Eq. (15), Young's modules of the concrete can be obtained as 29.99 GPa (39.30 MPa in strength), at least 36.62 GPa (at least 58.61 MPa in strength), and 30.77 GPa (41.37 MPa in strength) for the bridge deck, girders, and diaphragms, respectively. As can be seen, these rebounding hammer test results for the bridge deck and girders are very close to the updated results, which confirms the reliability of the updated results. Again, the difference of the diaphragm is due to the connection details, not the material itself.

The first three natural frequencies predicted using the updated parameters and their differences between the measured parameters are shown in Table 11. The maximum strains and maximum deflections on seven girders using the reconstructed model are also compared with those measured from field tests in Fig. 7. Again, the measured strain from G5 is not given in the figure because of an obvious error with the measurement data.

From Table 11 and Fig. 7, it can be seen that the reconstructed strains from the updated bridge model match the measured strains

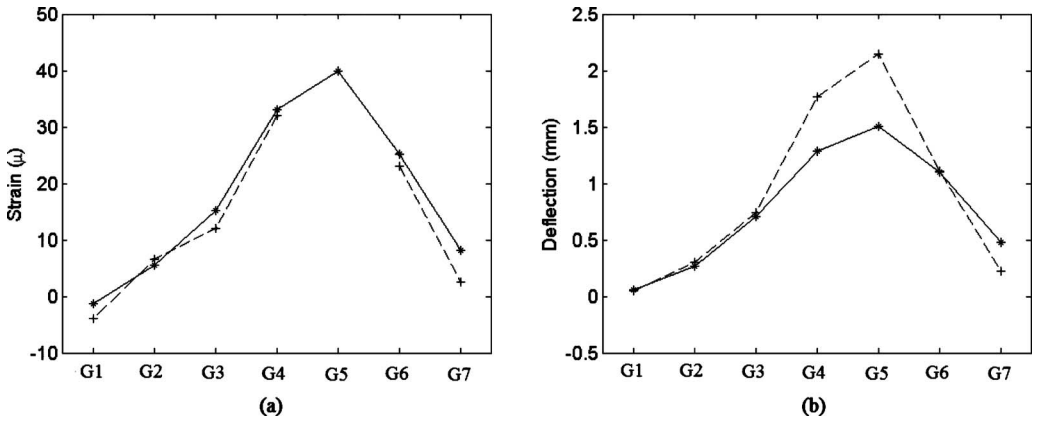

Fig. 7. Reconstructed and measured responses on the seven girders: (a) strains; (b) deflections (+−−, measured response; ∗ —, reconstructed response).

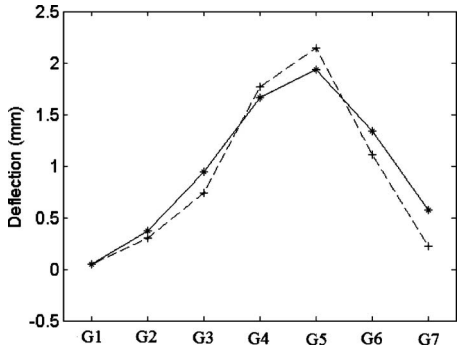

Fig. 8. Reconstructed and measured deflections on the seven girders when using deflections in model updating (+−−, measured response; ∗ —, reconstructed response).

from the field test very well, which demonstrates that the proposed RSM can be used to update the parameters efficiently. However, the match between the measured and reconstructed deflections in Fig. 7(b) is not as good as that of the strains in Fig. 7(a). A possible explanation could be that the strains are used in the objective function rather than the deflections. Therefore, it could be predicted that if deflections were used in the objective function, a better match-up could be achieved for deflections.

For the purpose of demonstration, the five parameters were also updated based on the natural frequencies and deflections of the seven girders, and the following updated results were obtained as 24.77 GPa, 27.67 GPa, 10.0 GPa, 2705 kg/m^3, and 33.06 MPa, respectively. Significant differences can be found between the two sets of updated parameters obtained with different objective functions. One possible reason for the differences could be that the measured deflections were larger than the true deflections of the seven girders since the deflection gauges were set on sand-evened surface instead of on a solid base. An overestimated deflection makes the updated bridge model more flexible, which results in a lower modulus of elasticity.

The comparison of the measurement and reconstructed deflection is shown in Fig. 8, and a good match is achieved. As was shown in a separate study where the updated model of the present study was used to identify dynamic vehicle wheel loads (Deng and Cai 2008), the vehicle axle loads can be identified based on either strain or deflection, as long as the corresponding updated model is used in the identification process. Therefore, based on different intensions of using the updated model, one can strategically choose different objective functions or change the weight of the variables.

Conclusion and Closing Remarks

A new, practical, user-friendly FE model updating method using the RSM and GA has been proposed. Parameters that need to be updated are first selected, and experimental design on the selected parameters can be optimized using the RSM. Structural responses are also selected based on the purpose of model updating. Numerical simulation can then be performed using the combinations of parameters from the experimental design, and structural responses can be obtained. RSFs for the structural responses can then be obtained by the regression method. Second-order RSFs are commonly used; however, sometimes third-order RSFs are needed to achieve sufficient accuracy. After that, an objective function can be built up using the residuals between the measured responses and the predicted responses from the built RSFs and can then be optimized to obtain the updated parameters using the GA.

The proposed methodology avoids developing sensitivity matrices and is much more convenient than a typical method reported in the literature. By employing second- or even higher-order polynomials, the RSM can model the curvature effects between the response and parameters which the sensitivity-based methods are not able to reflect. By adjusting the range for each parameter and adding or removing some cross terms or higher-order terms, appropriate RSFs with good accuracy and coverage of a large range of parameters can be obtained.

In order to successfully identify the parameters, the number of responses used in the objective function should not be less than the number of parameters. The proposed method has been applied to the model updating of a simulated beam as well as an existing bridge. Substantial agreement has been observed between the updated and real parameters for the simulated beam. For the existing bridge, the measured bridge responses and their reconstructed counterparts from the updated bridge model also match up very well, with reasonable explanations available for the updated parameters. However, to use the RSM for optimal experimental design efficiently, the number of parameters is usually limited to no more than eight. Experimental design involving more than eight parameters can be very complicated and the resulting RSFs can sometimes be difficult to interpret.

Acknowledgments

The writers are thankful to Louisiana State University for providing Economic Development Assistantship to L.D. and to the Louisiana DOTD and Louisiana Transportation Research Center for making the field test possible. The LaDOTD crew helped conduct the bridge field test. Special thanks go to Walid Alaywan for coordinating the test and Dr. Doc Zhang for providing the surface profiling test. Many graduate students and visiting scholars at LSU also helped prepare and carry out the bridge test. The constructive comments from the reviewers are also greatly appreciated.

References

AASHTO. (1998). *LRFD bridge design specification*, Washington, D.C.

AASHTO. (2004). *LRFD bridge design specification*, Washington, D.C.

Barker, M. G. (2001). "Quantifying field-test behavior for rating steel girder bridges." *J. Bridge Eng.*, 6(4), 254–261.

Baruch, M., and Bar-Itzhack, I. Y. (1978). "Optimal weighted orthogonalization of measured modes." *AIAA J.*, 16(4), 346–351.

Berman, A., and Nagy, E. J. (1983). "Improvement of large analytical model using test data." *AIAA J.*, 21(8), 1168–1173.

Brownjohn, J. M. W., and Xia, P. Q. (2000). "Dynamic assessment of curved cable-stayed bridge by model updating." *J. Struct. Eng.*, 126(2), 252–260.

Bucher, C. G., and Bourgund, U. (1990). "A fast and efficient response surface approach for structural reliability problems." *Struct. Safety*, 7, 57–66.

Cai, C. S., and Shahawy, M. (2004). "Predicted and measured performance of pre-stressed concrete bridges." *J. Bridge Eng.*, 9(1), 4–13.

Cheng, J., Cai, C. S., and Xiao, R. C. (2005). "Probabilistic shear-lag analysis of structures using systematic RSM." *Struct. Eng. Mech.*, 21(5), 507–518.

Cheng, J., Zhang, J., Cai, C. S., and Xiao, R. C. (2007). "A new approach

for solving inverse reliability problems with implicit response functions." *Eng. Struct.*, 29(1), 71–79.
Das, P. K., and Zheng, Y. (2000). "Cumulative formation of response surface and its use in reliability analysis." *Probab. Eng. Mech.*, 15(4), 309–315.
Deng, L., and Cai, C. S. (2008). "Identification of dynamic vehicular axle loads: Demonstration by a field of study." *J. Vib. Control* (to be published).
Doebling, S. W., Farrar, C. R., and Prime, W. B. (1998). "A summary review of vibration-based damage identification methods." *Shock Vib. Dig.*, 30(2), 91–105.
Friswell, M. I., and Mottershead, J. E. (1995). *Finite element model updating in structural dynamics*, Kluwer Academic, Dordrecht, The Netherlands.
Gen, M., and Cheng, R. (1997). *Genetic algorithms & engineering design*, John Wiley & Sons, Inc., New York.
Goldberg, D. E. (1989). *Genetic algorithms in search, optimization, and machine learning*, Addison-Wesley, Reading, Mass.
Hajela, P., and Soeilo, F. J. (1990). "Structural damage detection based on static and modal analysis." *AIAA J.*, 28(6), 1110–1115.
Hamed, E., and Frostig, Y. (2006). "Natural frequencies of bonded and unbonded prestressed beams-prestress force effects." *J. Sound Vib.*, 295, 28–39.
Jaishi, B., and Ren, W. X. (2005). "Structural finite element model updating using ambient vibration test results." *J. Struct. Eng.*, 131(4), 617–628.
Kutner, M. H., Nachtsheim, C. J., Neter, J., and Li, W. (2004). *Applied linear statistical models*, McGraw-Hill Companies, Inc., New York.
Landman, D., Simpson, J., Vicroy, D., and Parker, P. (2007). "Response surface methods for efficient complex aircraft configuration aerodynamic characterization." *J. Aircr.*, 44(4), 1189–1195.
Lee, P. K. K., Ho, D., and Chung, H. W. (1987). "Static and dynamic tests of concrete bridge." *J. Struct. Eng.*, 113(1), 61–73.
Link, M. (1999). "Updating of analytical models—Review of numerical procedures and application aspects." *Proc., Structural Dynamics Forum SD2000*,.
Marwala, T. (2004). "Finite element model updating using response surface method." *Collection of technical papers—AIAA/ASME/ASCE/AHS/ASC structures, structural dynamics and materials conference*, Vol. 7, 5165–5173.
Mazurek, D. F., and DeWolf, J. T. (1990). "Experimental study of bridge monitoring technique." *J. Struct. Eng.*, 116(9), 2532–2549.
Saiidi, M., Douglas, B., and Feng, S. (1994). "Prestress force effect on vibration frequency of concrete bridges." *J. Struct. Eng.*, 120(7), 2233–2241.
Salawu, O. S., and Williams, C. (1995). "Bridge assessment using forced-vibration testing." *J. Struct. Eng.*, 121(2), 161–172.
Sanayei, M., Imbaro, G. R., McClain, J. A. S., and Brown, L. C. (1997). "Structural model updating using experimental static measurements." *J. Struct. Eng.*, 123(6), 792–798.
Teughels, A., Maeck, J., and De Roeck, G. (2001). "A finite element model updating method using experimental modal parameters applied on a railway bridge." *Proc., 7th Int. Conf. on Computer Aided Optimum Design of Structures*, 97–106.
Wahab, M. M. A. (2001). "Effect of modal curvatures on damage detection using model updating." *Mech. Syst. Signal Process.*, 15(2), 439–445.
Wang, B. P., Han, Z. X., Xu, L., and Reinikainen, T. (2005). "A novel response surface method for design optimization of electronic packages." *Proc., 6th Int. Conf. on Thermal, Mechanical and Multi-Physics Simulation and Experiments in Micro-Electronics and Micro-Systems—EuroSimE 2005*, 175–181.
Wu, J. R., and Li, Q. S. (2004). "Finite element model updating for a high-rise structure based on ambient vibration measurements." *Eng. Struct.*, 26(7), 979–990.
Xia, P. Q., and Brownjohn, J. M. W. (2004). "Bridge structural condition assessment using systematically validated finite element model." *J. Bridge Eng.*, 9(5), 418–423.
Zhang, Q. W., Chang, C. C., and Chang, T. Y. P. (2001). "Finite element model updating for the Kap Shui Mun cable-stayed bridge." *J. Bridge Eng.*, 6(4), 285–293.
Zheng, Y., and Das, P. K. (2000). "Improved response surface method and its application to stiffened plate reliability analysis." *Eng. Struct.*, 22(5), 544–551.